A MESHFREE METHOD FOR ELASTICITY PROBLEMS WITH INTERFACES

NUNO F.M. MARTINS * AND MAGDA REBELO †

Abstract. In this work, we develop a meshfree method based on fundamental solutions basis functions for a transmission problem in linear elasticity. The problem here addressed, consists in computing the displacement field of an elastic object, which has piecewise constant Lamé coefficients, from a given displacement field on the boundary. The Lamé coefficients are assumed to be constant in non overlaping subdomains and, on the corresponding interface (interior boundaries), non homogeneous jump conditions on the displacement and on the traction vectors are considered. The main properties of the method are analyzed and illustrated with several numerical simulations in 2D domains.

Key words.
Meshfree methods, method of fundamental solutions, linear elasticity, transmission problems.

AMS subject classifications. MSC2010 65N80, 35J57, 35Q74.

1. Introduction. Meshfree methods are a class of numerical methods used in the construction of numerical approximations for several types of problems. These methods have interesting features. For instance, they are easy to implement (no mesh construction is required), provide accurate results and they deal well with more complex (two or three dimensional) geometries. These methods have been widely used to solve many boundary value problems and have also been used in other areas of research (see [6] for an overview and historical background on the subject).

There are several meshfree methods for PDE's and related boundary value problems. One possible approach is to consider the approximation represented as a linear combination of radial basis functions (RBF) centered at some chosen (source) points and then to compute the coefficents by imposing the PDE and boundary conditions at some collocation points. This is the main idea behind the so called Kansa's method (cf. [9]). If on one hand this leads to a densely defined and ill-conditioned system of linear equations on the other, the matrix can be very large (because we are imposing both the PDE and the boundary conditions). There are, however, cases where we can choose basis functions that are fitted to the PDE. For instance, for homogeneous elliptic problems with constant coefficients we have natural basis functions given by fundamental solutions of the underlying PDE. This particular choice of basis functions leads to the so called method of fundamental solutions (MFS). It is a meshfree boundary method (no domain collocation is required) and although it was recently extended to non homogeneous PDE's (cf. [3]), it has been mostly considered as a numerical method for homogeneous boundary value problems since the first papers by Kupradze and Alekside [10] or Oliveira [12]. More recently, the MFS has gained attention by the inverse problems community, mainly for Cauchy data reconstruction (see [7] for a survey on the subject). As point out by Alves (cf. [1], [2]), there is a strong connection between the MFS and RBF approximations. In fact, many RBF domain approximations are variations of the MFS in higher dimension. On the other hand, there is also a strong connection between the MFS for direct and Cauchy data

*Department of Mathematics, Facudade de Ciências e Tecnologia, Universidade Nova de Lisboa, Quinta da Torre, 2829-516 Caparica, Portugal (nfm@fct.unl.pt).

†Department of Mathematics, Facudade de Ciências e Tecnologia, Universidade Nova de Lisboa, Quinta da Torre, 2829-516 Caparica, Portugal (msjr@fct.unl.pt).

reconstruction (inverse) problems (eg. [4]). Therefore, fundamental basis functions are a good starting point for the development of meshfree approximation schemes in more general (direct or inverse) contexts.

In this paper, we propose a meshfree approximation using fundamental solutions basis functions for a direct linear elasticity problem with interfaces. These transmission problems arise often in several direct engineering problems, such as in materials science (see [13] and the references therein) and are also strongly connected to some inverse engineering problems, for instance in medical imaging (eg. [8]). The numerical study of such problems have been addressed by several authors, only in the 2D case, using finite element based methods (eg. [13], [14]). We shall consider here a more general situation of multiply interfaces in two or three dimensional cases.

We start with the formulation of the problem. Let Ω, $\omega_1, \ldots, \omega_m$ be open, bounded, regular (say, at least C^1) and simply connected (2D or 3D) domains, such that $\omega_i \subset\subset \Omega$ and $\overline{\omega}_i \cap \overline{\omega}_j = \emptyset$, $\forall i \neq j$. We shall denote the corresponding boundaries by $\gamma_0 := \partial\Omega$ and $\gamma_i := \partial\omega_i$. Define $\omega := \cup_i \omega_i$ and the multiply connected domain $\omega_0 := \Omega \setminus \overline{\omega}$ and note that

$$\partial\omega_0 = \gamma_0 \cup \gamma_1 \cup \ldots \cup \gamma_m.$$

The set Ω can be seen as a domain occupied by an elastic body with constant Lamé parameters, $\lambda_i, \mu_i > 0$ on each connected component ω_i. In the presence of body forces $f_i \in \mathbf{L}^2(\omega_i) := \left(L^2(\omega_i)\right)^d$ the governing system of equations is

$$\left\{ \begin{array}{ll} \nabla \cdot \sigma_i(\mathbf{u}) = \mathbf{f_i} & \text{in } \omega_i \\ \mathbf{u} = \mathbf{g}_0 & \text{on } \gamma_0 \\ [\mathbf{u}] = \mathbf{g}_i & \text{on } \gamma_i \\ \sigma_0(\mathbf{u})n - \sigma_i(\mathbf{u})n = \mathbf{g}_i^n & \text{on } \gamma_i \end{array} \right. \tag{1.1}$$

where the stress tensor σ_i is defined (in terms of the displacement vector $\mathbf{u}$) by

$$\sigma_i(\mathbf{u}) = \lambda_i(\nabla \cdot \mathbf{u})I + \mu_i(\nabla\mathbf{u} + \nabla\mathbf{u}^\top).$$

Notice that

$$\nabla \cdot \sigma_i(\mathbf{u}) = \mu_i \Delta\mathbf{u} + (\lambda_i + \mu_i)\nabla\nabla\mathbf{u}$$

where $\Delta\mathbf{u} = (\Delta u_1, \ldots, \Delta u_d)$ and $\sigma_i(\mathbf{u})n$ is the surface traction vector on the interface γ_i, where n is the outward normal vector with respect to ω_0 (hence, pointing inwards with respect to $\omega_1, \ldots, \omega_m$). The jump $[\mathbf{u}]$ on the interface γ_i is defined by $\mathbf{u}^+ - \mathbf{u}^-$, where $\mathbf{u}^+$ is the trace of $\mathbf{u}$ coming from ω_0 and $\mathbf{u}^-$ is the trace of $\mathbf{u}$ coming from ω_i. The last boundary condition is the normal jump of $\mathbf{u}$ across γ_i defined in terms of the normal trace $\sigma_0(\mathbf{u})n$ coming from ω_0 and the normal trace $\sigma_i(\mathbf{u})n$ coming from ω_i.

The problem that we shall address is to, given the geometry $\Omega, \omega_0, \ldots, \omega_m$, the Lamé parameters λ_i, μ_i, the source terms $\mathbf{f}_i$ and the boundary data $\mathbf{g}_i$ and $\mathbf{g}_i^n$, compute the solution, $\mathbf{u}$ of the above system of partial differential equations.

It is well known that, this problem is well posed, with $\mathbf{u} \in \mathbf{H}^1(\Omega) = \left(H^1(\Omega)\right)^d$. In this setting, $\mathbf{g}_i \in \mathbf{H}^{1/2}(\gamma_i) = \left(H^{1/2}(\gamma_i)\right)^d$ and $\mathbf{g}_i^n \in \mathbf{H}^{-1/2}(\gamma_i) = \left(H^{-1/2}(\gamma_i)\right)^d$.

2. Meshfree collocation method.

A common approach in meshfree methods is to consider some (vectorial) basis functions ζ_k^i and represent the solution as

$$\widetilde{\mathbf{u}}_i(x) = \widetilde{\mathbf{u}}|_{\omega_i}(x) = \sum_k \alpha_k^i \zeta_k^i(x), \quad \forall x \in \omega_i$$

where the coefficients $\alpha_k^i \in \mathbb{R}^d$ are computed by imposing, on some collocation points,

$$\begin{cases} \sum_k \alpha_k^i \left(\nabla \cdot \sigma_i(\zeta_k^i)\right)(x_l^i) = \mathbf{f_i}(x_l^i) & x_l^i \in \omega_i \\ \sum_k \alpha_k^0 \zeta_k^0(x_l^{\gamma_0}) = \mathbf{g}_0(x_l^{\gamma_0}) & x_l^{\gamma_0} \in \gamma_0 \\ \sum_k \alpha_k^0 \zeta_k^0(x_l^{\gamma_0}) - \sum_k \alpha_k^i \zeta_k^i(x_l^{\gamma_i}) = \mathbf{g}_i(x_l^{\gamma_i}) & x_l^{\gamma_i} \in \gamma_i \\ \sum_k \alpha_k^0 \left(\sigma_0\left(\zeta_k^0\right)(x_l^{\gamma_i}) n_{x_l^{\gamma_i}}\right) - \sum_k \alpha_k^i \left(\sigma_i\left(\zeta_k^i\right)(x_l^{\gamma_i}) n_{x_l^{\gamma_i}}\right) = \mathbf{g}_i^n(x_l^{\gamma_i}) & x_l^{\gamma_i} \in \gamma_i \end{cases} . \tag{2.1}$$

The first set of equations,

$$\sum_k \alpha_k^i \left(\nabla \cdot \sigma_i(\zeta_k^i)\right)(x_l^i) = \mathbf{f_i}(x_l^i), \quad x_l^i \in \omega_i \tag{2.2}$$

are domain equations, and are imposed in order to satisfy the PDE. The last set of (boundary) equations

$$\begin{cases} \sum_k \alpha_k^0 \zeta_k^0(x_l^{\gamma_0}) = \mathbf{g}_0(x_l^{\gamma_0}) & x_l^{\gamma_0} \in \gamma_0 \\ \sum_k \alpha_k^0 \zeta_k^0(x_l^{\gamma_0}) - \sum_k \alpha_k^i \zeta_k^i(x_l^{\gamma_i}) = \mathbf{g}_i(x_l^{\gamma_i}) & x_l^{\gamma_i} \in \gamma_i \\ \sum_k \alpha_k^0 \left(\sigma_0\left(\zeta_k^0\right)(x_l^{\gamma_i}) n_{x_l^{\gamma_i}}\right) - \sum_k \alpha_k^i \left(\sigma_i\left(\zeta_k^i\right)(x_l^{\gamma_i}) n_{x_l^{\gamma_i}}\right) = \mathbf{g}_i^n(x_l^{\gamma_i}) & x_l^{\gamma_i} \in \gamma_i \end{cases} \tag{2.3}$$

are imposed in order to fit the boundary data.

If on one hand, the chosen basis functions must be able to give a good approximation to the solution of the problem (for instance should span a dense subset in the space where the solution is sought), on the other it should also simplify the above system of equations. For instance, if we take basis functions ζ_k^i with the eigenvalue property

$$\nabla \cdot \sigma_i(\zeta_k^i) = -\kappa_k^i \zeta_k^i,$$

then, the domain equations on the above system simplifies to the linear equations

$$\sum_k \alpha_k^i \kappa_k^i \zeta_k^i(x_l^i) = \mathbf{f_i}(x_l^i). \tag{2.4}$$

There are several basis functions with the above eigenvalue property. Take, for instance, in the 2D case, the basis functions (see [5])

$$\mathbf{\Psi}_y^{\kappa_k^i} e_1 \text{ and } \mathbf{\Psi}_y^{\kappa_k^i} e_2, \quad y \notin \overline{\omega}_i,$$

where $\mathbf{\Psi}_y^{\kappa_k^i}$ $(\kappa_k^i > 0)$ is the fundamental tensor centered at y,

$$\mathbf{\Psi}_y^{\kappa_k^i}(x) = \frac{\mathbf{i}}{4\kappa_k^i} \left[\frac{\kappa_k^i}{\mu_k^i} H_1^{(0)}\left(\sqrt{\frac{\kappa_k^i}{\mu_k^i}}|x-y|\right) \delta_{ij} + \frac{\partial^2 \left(H_1^{(0)}\left(\sqrt{\frac{\kappa_k^i}{\mu_k^i}}|x-y|\right) - H_1^{(0)}\left(\sqrt{\frac{\kappa_k^i}{\lambda_k^i+2\mu_k^i}}|x-y|\right)\right)}{\partial x_i \partial x_j} \right],$$

for the elastodynamic system $\nabla \cdot \sigma_i(\mathbf{u}) + \kappa_k^i \mathbf{u} = 0$. Recall that a fundamental solution for the elastodynamic equations satisfies

$$\nabla \cdot \sigma_i(\mathbf{\Psi}_y^{\kappa_k^i}) + \kappa_k^i \mathbf{\Psi}_y^{\kappa_k^i} = -\delta_y I,$$

where δ_y is the Dirac delta distribution centered at y.

However, even with the above simplification, the system (2.1) may become very large. One way to deal with this is to split the solution as $\mathbf{u} = \mathbf{u}_P + \mathbf{u}_H$. On a first step, we determine a particular solution $\nabla \cdot \sigma_i(\mathbf{u}_P) = \mathbf{f}_i$. This can be achieved by solving, for instance, a system of linear domain equations similar to (2.2). On a second step, we determine $\mathbf{u}_H = \mathbf{u} - \mathbf{u}_P$ by solving the homogeneous problem

$$\begin{cases} \nabla \cdot \sigma_i(\mathbf{u}_H) = 0 & \text{in } \omega_i \\ \mathbf{u_H} = \mathbf{g}_0 - \mathbf{u}_P & \text{on } \gamma_0 \\ [\mathbf{u}_H] = \mathbf{g}_i - [\mathbf{u}_P] & \text{on } \gamma_i \\ \sigma_0(\mathbf{u}_H)n - \sigma_i(\mathbf{u}_H)n = \mathbf{g}_i^n - \sigma_0(\mathbf{u}_P)n + \sigma_i(\mathbf{u}_P)n & \text{on } \gamma_i \end{cases}.$$

Taking an appropriate choice of basis functions, we can reduce the problem to a system of boundary linear equations, similar to (2.3).

Henceforth, we focus on this last problem, which, can be generically described as to compute $\mathbf{v}$ such that

$$\begin{cases} \nabla \cdot \sigma_i(\mathbf{v}) = 0 & \text{in } \omega_i \\ \mathbf{v} = \mathbf{h}_0 & \text{on } \gamma_0 \\ [\mathbf{v}] = \mathbf{h}_i & \text{on } \gamma_i \\ \sigma_0(\mathbf{v})n - \sigma_i(\mathbf{v})n = \mathbf{h}_i^n & \text{on } \gamma_i \end{cases}. \tag{2.5}$$

3. The MFS for elasticity problems with interfaces. In the above case, a natural choice of basis functions is given in terms of the fundamental tensor for the Lamé system (see [5])

$$\mathbf{\Phi}^i(x) = \begin{cases} \dfrac{\lambda_i + 3\mu_i}{4\pi\mu_i(\lambda_i + 2\mu_i)} \left[-\ln|x|\delta_{ij} + \dfrac{\lambda_i + \mu_i}{\lambda_i + 3\mu_i} \dfrac{x_j x_k}{|x|^2} \right]_{1 \le j,k \le 2} & x \in \mathbb{R}^2 \setminus \{0\} \\ \dfrac{\lambda_i + 3\mu_i}{8\pi\mu_i(\lambda_i + 2\mu_i)} \left[\dfrac{1}{|x|}\delta_{ij} + \dfrac{\lambda_i + \mu_i}{\lambda_i + 3\mu_i} \dfrac{x_j x_k}{|x|^3} \right]_{1 \le j,k \le 3} & x \in \mathbb{R}^3 \setminus \{0\} \end{cases}. \tag{3.1}$$

Taking linear combinations

$$\widetilde{\mathbf{v}}_i(x) = \widetilde{\mathbf{v}}|_{\omega_i}(x) = \sum_k \mathbf{\Phi}_{y_k^i}^i(x)\alpha_k^i, \quad \forall x \in \omega_i, \quad y_k^i \notin \overline{\omega}_i \tag{3.2}$$

where $\alpha_k^i \in \mathbb{R}^d$ and $\mathbf{\Phi}_y^i := \mathbf{\Phi}^i(\bullet - y)$ is the point source tensor, we have

$$\nabla \cdot \sigma_i(\widetilde{\mathbf{v}}_i) = 0 \ \text{ in } \ \omega_i. \tag{3.3}$$

Note that $\widetilde{\mathbf{v}}_i$ is pointwise defined (and smooth) in $\mathbb{R}^d \setminus \{y_1^i, \ldots, y_{n_i}^i\} \supset \overline{\omega}_i$. Therefore, the corresponding boundary linear system (2.3) is well defined and from here we can compute the coefficients α_k^i. Next result shows that the basis functions in equation (3.2) are linearly independent.

LEMMA 3.1. *The set*

$$\left\{\mathbf{\Phi}^i_{y_1},\ldots,\mathbf{\Phi}^i_{y_p}\right\}$$

with $y_j \neq y_k, \forall j \neq k$ *is linearly independent in* $\mathbb{R}^d \setminus \{y_1,\ldots,y_p\}$.

Proof. Suppose that

$$\mathbf{u} := \mathbf{\Phi}^i_{y_1}\alpha_1 + \ldots + \mathbf{\Phi}^i_{y_p}\alpha_p = 0 \text{ in } \mathbb{R}^d \setminus \{y_1,\ldots,y_p\}.$$

Take a regular domain Ω, such that $y_k \in \Omega$ and $y_1,\ldots,y_{k-1},y_{k+1},\ldots,y_p \notin \overline{\Omega}$. Then,

$$\begin{cases} \nabla\cdot\sigma_i(\mathbf{u}) = -\delta_{y_k}\alpha_k & \text{in } \Omega \\ \mathbf{u} = 0 & \text{on } \partial\Omega \\ \sigma_i(\mathbf{u})\,n = 0 & \text{on } \partial\Omega \end{cases}.$$

From Betti's formula,

$$\int_\Omega (\nabla\cdot\sigma_i(\mathbf{u})\cdot\mathbf{w} - \mathbf{u}\cdot\nabla\cdot\sigma_i(\mathbf{w}))\,dx = \int_{\partial\Omega}(\sigma_i(\mathbf{u})n\cdot\mathbf{w} - \mathbf{u}\cdot\sigma_i(\mathbf{w})n)\,dS_x.$$

In particular, for $\mathbf{w}_l = e_l$ we have

$$-\alpha_k\cdot e_l = \int_\Omega ((\nabla\cdot\sigma_i(\mathbf{u}))\cdot\mathbf{w}_l - \mathbf{u}\cdot(\nabla\cdot\sigma_i(\mathbf{w}_l)))\,dx = 0.$$

□

Since the approximation $\widetilde{\mathbf{v}}$ satisfies equation (3.3) and the transmission problem (2.5) is well posed with $\mathbf{v}\in\mathbf{H}^1(\Omega)$ it is clear that if the trace and normal trace of $\widetilde{\mathbf{v}}$ provides a good approximation of the boundary data (in appropriate trace spaces) then $\widetilde{\mathbf{v}}$ provides a good approximation for $\mathbf{v}$ in the $\mathbf{H}^1(\Omega)$ sense.

From the above discussion, the MFS approximation requires that source points y^i_k should be placed outside $\overline{\omega}_i$. From the theoretical point of view, there are several possible choices for the location of source points (eg. [2]). However, in practise, considering point sources located on artificial boundaries enclosing the domain of interest provides better numerical results. We shall consider this approach.

Let $\widetilde{\Omega}$ be an artificial regular domain (bounded, open and simply connected) enclosing Ω, that is, $\Omega \subset\subset \widetilde{\Omega}$. Consider also the artificial domains $\widetilde{\Omega}_i$ such that $\omega_i \subset\subset \widetilde{\Omega}_i$, $i=1,\ldots,m$ and $\overline{\widetilde{\Omega}}_i \cap \overline{\widetilde{\Omega}}_k = \emptyset$ so that each non overlapping domain $\widetilde{\Omega}_i$ encloses ω_i. Since ω_0 is multiply connected (it has m holes $\omega_1,\ldots,\omega_m$), we must also consider artificial domains, $\widetilde{\omega}_i$, inside ω_i $(i=1,\ldots,m)$ and put

$$\widetilde{\omega}_0 := \widetilde{\Omega}\setminus\left(\overline{\widetilde{\omega}}_1\cup\ldots\cup\overline{\widetilde{\omega}}_m\right).$$

The source points will be considered on the boundaries $\widetilde{\Gamma}_i := \partial\widetilde{\Omega}_i$, $\widetilde{\gamma}_i := \partial\widetilde{\omega}_i$ $(i=1,\ldots,m)$ and on $\widetilde{\gamma}_0 := \partial\widetilde{\Omega}$ (see Fig. 3.1).

This means that numerical approximations (3.2) can now be written as

$$\widetilde{\mathbf{v}}_0(x) = \sum \mathbf{\Phi}^0(x-y^0_j)\alpha^0_j, \quad y^0_j\in\partial\widetilde{\omega}_0, \tag{3.4}$$

$$\widetilde{\mathbf{v}}_i(x) = \sum \mathbf{\Phi}^i(x-y^i_j)\alpha^i_j, \quad y^i_j\in\widetilde{\Gamma}_i. \tag{3.5}$$

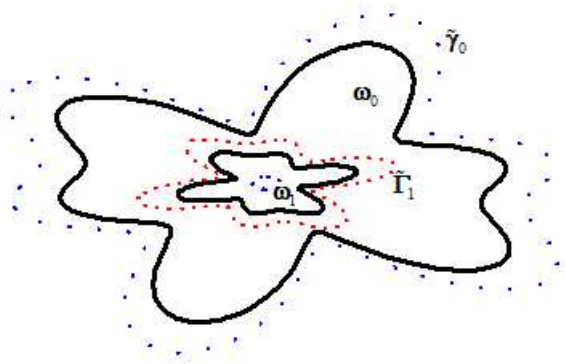

FIG. 3.1. *Source points scheme in a domain with one interface. Full lines are the boundary of the domain, dotted lines are the artificial boundaries.*

The corresponding boundary equations are

$$\begin{cases} \sum_j \mathbf{\Phi}^0_{y^0_j} \alpha^0_j = \mathbf{h}_0 \\ \sum_j \mathbf{\Phi}^0_{y^0_j} \alpha^0_j - \sum_j \mathbf{\Phi}^i_{y^i_j} \alpha^i_j = \mathbf{h}_i \\ \sum_j \sigma_0 \left(\mathbf{\Phi}^0_{y^0_j} \right) n \alpha^0_j - \sum_j \sigma_i \left(\mathbf{\Phi}^i_{y^i_j} \right) n \alpha^i_j = \mathbf{h}^n_i \end{cases} . \tag{3.6}$$

PROPOSITION 3.2. *Given the input data* $(\mathbf{h}_0, \ldots, \mathbf{h}_m, \mathbf{h}^n_1, \ldots, \mathbf{h}^n_m)$ *and source points* y^i_j *in the previous conditions, system (3.6) has at most one solution.*

Proof. Since the above problem is linear, it is sufficient to show that the kernel of the associated operator is null. Suppose that

$$(\mathbf{h}_0, \ldots, \mathbf{h}_m, \mathbf{h}^n_1, \ldots, \mathbf{h}^n_m) = (0, \ldots, 0) .$$

Then, function $\widetilde{\mathbf{v}} \in \mathbf{H}^1(\Omega)$ defined by (3.4) and (3.5) satisfies (2.5) with null input boundary data. By well posedness of this problem, we must have

$$\widetilde{\mathbf{v}}_i = 0 \text{ in } \omega_i.$$

By analytic continuation, $\widetilde{\mathbf{v}}_i = 0$ in $\mathbb{R}^d \setminus \left\{ y^i_1, \ldots, y^i_k \right\}$ and from lemma 3.1 follows

$$\alpha^i_1 = \ldots = \alpha^i_m = 0.$$

□

The following results concerns the approximation properties of the fundamental basis functions for the given boundary conditions. In order to study these properties, we start by defining the single layer representations (see [11] for notation)

$$\mathbf{u}_0(x) = \sum_{i=0}^{m} SL_{\tilde{\gamma}_i}(\psi_i)(x) \tag{3.7}$$

$$\mathbf{u}_i(x) = SL_{\tilde{\Gamma}_i}(\phi_i)(x), \quad i = 1, \ldots, m \tag{3.8}$$

where

$$SL_{\widetilde{\gamma}_i}(\psi_i)(x) = \int_{\widetilde{\gamma}_i} \mathbf{\Phi}^0_x(y)\psi_i(y)dS_y,\ x \in \mathbb{R}^d \setminus \widetilde{\gamma}_i$$

and

$$SL_{\widetilde{\Gamma}_i}(\phi_i)(x) = \int_{\widetilde{\Gamma}_i} \mathbf{\Phi}^i_x(y)\phi_i(y)dS_y,\ x \in \mathbb{R}^d \setminus \widetilde{\Gamma}_i.$$

The kernel of the above operators is the point source tensor (3.1) and $\psi_i = (\psi_i^1, \ldots, \psi_i^d)$, $\phi_i = (\phi_i^1, \ldots, \phi_i^d)$ are integrable densities. Note that, by discretizing the above integrals we obtain a representation as in (3.2).

Since we are considering boundary data

$$\mathbf{h} = (\mathbf{h}_0, \ldots, \mathbf{h}_m) \in \mathbf{H}^{1/2}(\gamma) := \mathbf{H}^{1/2}(\gamma_0) \times \ldots \times \mathbf{H}^{1/2}(\gamma_m)$$

and

$$\mathbf{h}^n = (\mathbf{h}_1^n, \ldots, \mathbf{h}_m^n) \in \mathbf{H}^{-1/2}(\gamma \setminus \gamma_0) := \mathbf{H}^{-1/2}(\gamma_1) \times \ldots \times \mathbf{H}^{-1/2}(\gamma_m)$$

(so that transmission problem (2.5) is well posed in $\mathbf{H}^1(\Omega)$) then the proper functional framework for the densities is

$$\psi = (\psi_0, \ldots, \psi_m) \in \mathbf{H}^{-1/2}(\widetilde{\gamma}) := \mathbf{H}^{-1/2}(\widetilde{\gamma}_0) \times \ldots \times \mathbf{H}^{-1/2}(\widetilde{\gamma}_m)$$

and

$$\phi = (\phi_1, \ldots, \phi_m) \in \mathbf{H}^{-1/2}(\widetilde{\Gamma}) := \mathbf{H}^{-1/2}(\widetilde{\Gamma}_1) \times \ldots \times \mathbf{H}^{-1/2}(\widetilde{\Gamma}_m).$$

Therefore, the above single layer potentials must be understood in the duality sense. Notice that,

$$\nabla \cdot \sigma_0(\mathbf{u}_0) = 0 \ \text{ in } \mathbb{R}^d \setminus (\widetilde{\gamma}_0 \cup \widetilde{\gamma}_1 \cup \ldots \cup \widetilde{\gamma}_m)$$

and, for $i \geq 1$,

$$\nabla \cdot \sigma_i(\mathbf{u}_i) = 0 \ \text{ in } \mathbb{R}^d \setminus \widetilde{\Gamma}_i.$$

The system of boundary equations (3.6) is now given by the following integral equations

$$\text{(3.9)} \qquad \begin{cases} \displaystyle\sum_{j=0}^{m} SL_{\widetilde{\gamma}_j,\gamma_0}(\psi_j) = \mathbf{h}_0 \\ \displaystyle\sum_{j=0}^{m} SL_{\widetilde{\gamma}_j,\gamma_i}(\psi_j) - SL_{\widetilde{\Gamma}_i,\gamma_i}(\phi_i) = \mathbf{h}_i \\ \displaystyle\sum_{j=0}^{m} NSL_{\widetilde{\gamma}_j,\gamma_i}(\psi_j) - NSL_{\widetilde{\Gamma}_i,\gamma_i}(\phi_i) = \mathbf{h}_i^n \end{cases},$$

where $SL_{\widetilde{\Gamma}_0,\gamma_0}$ is the trace of $SL_{\widetilde{\Gamma}_0}$ on γ_0 and $NSL_{\widetilde{\Gamma}_1,\gamma_1}$ the normal trace of $SL_{\widetilde{\Gamma}_1}$ on γ_1, that is,

$$NSL_{\widetilde{\Gamma}_1,\gamma_1}(\phi_1)(x) = \int_{\widetilde{\Gamma}_1} \sigma_1(\mathbf{\Phi}^1_x(y))n_x\phi_1(y)dS_y,\ x \in \gamma_1.$$

Define the linear bounded operator

$$\mathbb{M} : \mathbf{H}^{-1/2}(\widetilde{\gamma}) \times \mathbf{H}^{-1/2}(\widetilde{\Gamma}) \to \mathbf{H}^{1/2}(\gamma) \times \mathbf{H}^{-1/2}(\gamma \setminus \gamma_0)$$

by

$$\mathbb{M}(\psi,\phi) := \begin{bmatrix} \displaystyle\sum_{j=0}^{m} SL_{\widetilde{\gamma}_j,\gamma_0}(\psi_j) \\ \displaystyle\sum_{j=0}^{m} SL_{\widetilde{\gamma}_j,\gamma_i}(\psi_j) - SL_{\widetilde{\Gamma}_i,\gamma_i}(\phi_i) \\ \displaystyle\sum_{j=0}^{m} NSL_{\widetilde{\gamma}_j,\gamma_i}(\psi_j) - NSL_{\widetilde{\Gamma}_i,\gamma_i}(\phi_i) \end{bmatrix}.$$

Clearly, system (3.9) is solvable if and only if $(\mathbf{h}, \mathbf{h}^n) \in$ Range $\mathbb{M}$.

In the following, we shall address the two dimensional case. In such case, we must consider the subspaces

$$\widehat{\mathbf{H}}^{1/2}(\gamma) = \left\{ \psi = (\psi_0, \ldots, \psi_m) \in \mathbf{H}^{1/2}(\gamma) : \int_{\gamma_i} \psi_i(x)dS_x = 0 \right\}$$

which can be identified to $\mathbf{H}^{1/2}(\gamma)/\mathbb{R}^2$ via the mapping

$$\mathbf{H}^{1/2}(\gamma) \ni \psi \mapsto \left(\psi_0 - \frac{1}{|\gamma_0|}\int_{\gamma_0} \psi_0(x)dS_x, \ldots, \psi_m - \frac{1}{|\gamma_m|}\int_{\gamma_m} \psi_m(x)dS_x \right) \in \widehat{\mathbf{H}}^{1/2}(\gamma)$$

for each $\psi \in \mathbf{H}^{1/2}(\gamma)$.

As we shall see in the following results, these subspaces are needed in the 2D case because of the asymptotic behavior of the fundamental tensor. This can be avoided by considering other artificial domain $\widetilde{\Omega}$ (for instance, adding an extra exterior artificial boundary). In the 3D case, the fundamental tensor has the appropriate asymptotic behavior, hence there is no need to consider other topology for $\widetilde{\Omega}$ nor to add constants.

PROPOSITION 3.3. *The restriction of* $\mathbb{M}$ *to* $\widehat{\mathbf{H}}^{-1/2}(\widetilde{\gamma}) \times \widehat{\mathbf{H}}^{-1/2}(\widetilde{\Gamma})$ *is injective.*

Proof. This proposition is similar to Proposition 3.2. However, in this boundary layer framework, we can not use the same arguments. Consider the layer representations (3.7) and (3.8), where the densities $\phi = (\phi_1, \ldots, \phi_m)$ and $\psi = (\psi_0, \ldots, \psi_m)$ belong to $\ker \mathbb{M}$. In particular, $\mathbf{u}$ satisfies problem (2.5) with boundary data $(\mathbf{h}, \mathbf{h}^n) = (0, 0)$. By well posedness of this problem, $\mathbf{u}_i = 0$ in ω_i, hence, by analytic continuation, $\mathbf{u}_0 = 0$ in $\widetilde{\omega}_0$ and $\mathbf{u}_i = 0$ in $\widetilde{\Omega}_i$. On the other hand, the single layer representations (3.7) and (3.8) imply the following jump relations

$$[\mathbf{u}_i]|_{\partial\widetilde{\omega}_i} = 0, \quad [\sigma_0(\mathbf{u}_0)n]|_{\widetilde{\gamma}_i} = \psi_i, \ \ [\sigma_i(\mathbf{u}_i)n]|_{\widetilde{\Gamma}_i} = \phi_i$$

and, in particular, follows $\mathbf{u}_0 = 0$ on $\partial\widetilde{\omega}_0$ (coming from the exterior of $\widetilde{\omega}_0$).

Since the asymptotic behavior of $\cong_0$ is (eg. [5])

$$\mathbf{u}_0(x) = c_0 \left(\sum_{j=0}^{m} \int_{\widetilde{\gamma}_j} \psi_j(y)dS_y \right) \log|x| + O(1), \qquad |x| \to \infty$$

where $c_0 = -\frac{\lambda_0+3\mu_0}{4\pi\mu_0(\lambda_0+2\mu_0)}$ and, by hypothesis,

$$\int_{\widetilde{\gamma}_i} \psi_i(y) d\sigma_y = 0$$

then, on the unbounded component $\mathbb{R}^2 \setminus \overline{\overline{\Omega}}$, we have

$$\begin{cases} \nabla \cdot \sigma_0(\mathbf{u}_0) = 0 & \text{in } \mathbb{R}^2 \setminus \overline{\overline{\Omega}} \\ \mathbf{u}_0 = 0 & \text{on } \widetilde{\gamma}_0 \\ \mathbf{u}_0(x) = O(1) & |x| \to \infty \end{cases}.$$

This problem is well posed in $\mathbf{H}^1_{loc}(\mathbb{R}^2 \setminus \overline{\overline{\Omega}})$ therefore, $\mathbf{u}_0 = 0$ in $\mathbb{R}^2 \setminus \overline{\overline{\Omega}}$. Also,

$$\begin{cases} \nabla \cdot \sigma_0(\mathbf{u}_0) = 0 & \text{in } \widetilde{\omega}_i \\ \mathbf{u}_0 = 0 & \text{on } \widetilde{\gamma}_i \end{cases}$$

and this implies $\mathbf{u}_0 = 0$ in $\widetilde{\omega}_i$. From this, we conclude that $\mathbf{u}_0 = 0$ in $\mathbb{R}^2 \setminus (\widetilde{\gamma}_0 \cup \ldots \cup \widetilde{\gamma}_m)$. In the same way, $\mathbf{u}_i = 0$ in $\mathbb{R}^2 \setminus \widetilde{\Gamma}_i$ and since the densities ϕ, ψ are the jumps of the normal derivative across the corresponding boundaries we have $(\phi, \psi) = (0, 0)$. □

We now show that, each set of input data $(\mathbf{h}, \mathbf{h}^n) \in \mathbf{H}^{1/2}(\gamma) \times \mathbf{H}^{-1/2}(\gamma \setminus \gamma_0)$ can be approximated by a sequence of the form $\mathbb{M}(\psi^n, \phi^n)$ (modulo constants, in the 2D case). In order to prove this result, we must consider the adjoint of $\mathbb{M}$. In this case, we have (see [4])

$$\mathbb{M}^* : \mathbf{H}^{-1/2}(\gamma) \times \mathbf{H}^{1/2}(\gamma \setminus \gamma_0) \to \mathbf{H}^{1/2}(\widetilde{\gamma}) \times \mathbf{H}^{1/2}(\widetilde{\Gamma})$$

given by

$$\mathbb{M}^*(\psi, \phi) = \begin{bmatrix} \sum_{j=0}^m SL_{\gamma_j, \widetilde{\gamma}_i}(\psi_j) + \sum_{j=1}^m DL_{\gamma_j, \widetilde{\gamma}_i}(\phi_j) \\ \\ -SL_{\gamma_i, \widetilde{\Gamma}_i}(\psi_i) - DL_{\gamma_i, \widetilde{\Gamma}_i}(\phi_i) \end{bmatrix},$$

where $SL_{\gamma_j, \widetilde{\gamma}_i}$ and $SL_{\gamma_i, \widetilde{\Gamma}_i}$ have the same meaning as above, but with kernel $\mathbf{\Phi}^0_x$ and $\mathbf{\Phi}^i_x$, respectively. The operator DL_{γ_j} is the double layer potential

$$DL_{\gamma_j}(\phi_j)(x) = \int_{\gamma_j} \mathbf{K}(x, y) \phi_j(y) dS_y$$

and $DL_{\gamma_j, \widetilde{\gamma}_i}$, $DL_{\gamma_j, \widetilde{\Gamma}_j}$ are the trace of DL_{γ_j} on $\widetilde{\gamma}_i$ and $\widetilde{\Gamma}_j$ with kernels $\mathbf{K}(x, y)$ given by $\sigma_0\left(\Phi^0_x\right)(y) n_y$ and $\sigma_j\left(\Phi^j_x\right)(y) n_y$, respectively.

PROPOSITION 3.4. *The restriction of* $\mathbb{M}^*$ *to* $\widehat{\mathbf{H}}^{-1/2}(\gamma) \times \widehat{\mathbf{H}}^{1/2}(\gamma \setminus \gamma_0)$ *is injective.*

Proof. Let $(\psi, \phi) \in \widehat{\mathbf{H}}^{-1/2}(\gamma) \times \widehat{\mathbf{H}}^{1/2}(\gamma \setminus \gamma_0)$ and suppose that $(\psi, \phi) \in \ker \mathbb{M}^*$. Define the following combination of single and double layers

$$\mathbf{u}_0 = \sum_{j=0}^m SL_{\gamma_j}(\psi_j) + \sum_{j=1}^m DL_{\gamma_j}(\phi_j)$$

and

$$\mathbf{u}_i = SL_{\gamma_i}(-\psi_i) + DL_{\gamma_i}(-\phi_i).$$

Clearly,

$$\nabla \cdot \sigma_0(\mathbf{u}_0) = 0 \text{ in } \mathbb{R}^2 \setminus (\gamma_0 \cup \ldots \cup \gamma_m)$$

and by hypothesis, $\mathbf{u}_0 = 0$ on $\widetilde{\gamma}_0 \cup \ldots \cup \widetilde{\gamma}_m$. Therefore, $\mathbf{u}_0 = 0$ in $\mathbb{R}^2 \setminus \overline{\omega}_0$. By the jump relations, we must have

$$0 = [\mathbf{u}_0]|_{\gamma_0} = \mathbf{u}_0^-|_{\gamma_0}, \quad \psi_j = [\sigma_0(\mathbf{u}_0)n]|_{\gamma_j} = \sigma_0(\mathbf{u}_0)n^-|_{\gamma_j}, \quad -\phi_j = [\mathbf{u}_0]|_{\gamma_j} = \mathbf{u}_0^-|_{\gamma_j}, \quad j = 1, \ldots, m.$$

On the other hand, $\mathbf{u}_j = 0$ in $\mathbb{R}^2 \setminus \overline{\omega}_j$ and from this we get the jumps

$$-\psi_j = [\sigma_j(\mathbf{u}_j)n]|_{\gamma_j} = -\sigma_j(\mathbf{u}_j)n^-|_{\gamma_j}, \quad -\phi_j = [\mathbf{u}_j]|_{\gamma_j} = \mathbf{u}_j^-|_{\gamma_j}$$

because the normal vector points inwards with respect to ω_j. From the above equations, we can write

$$\begin{cases} \nabla \cdot \sigma_0(\mathbf{u}_0) = 0 & \text{in } \omega_0 \\ \mathbf{u}_0 = 0 & \text{on } \gamma_0 \\ \mathbf{u}_0 - \mathbf{u}_j = 0 & \text{on } \gamma_j \\ \sigma_0(\mathbf{u}_0)n - \sigma_j(\mathbf{u}_j)n = 0 & \text{on } \gamma_j \\ \nabla \cdot \sigma_j(\mathbf{u}_j) = 0 & \text{in } \omega_j \end{cases}$$

and so, $\mathbf{u}_i = 0$ in ω_i. From here, we conclude that $\psi = \phi = 0$. □

4. Numerical Results. In order to illustrate the theoretical results of Section 3 we present several examples for the 2D-problem transmission problem (2.5) with a single interface

$$\begin{cases} \nabla \cdot \sigma_0(\mathbf{u}_0) = 0 & \text{in } \omega_0 \\ \nabla \cdot \sigma_1(\mathbf{u}_1) = 0 & \text{in } \omega_1 \\ \mathbf{u} = \mathbf{g}_0 & \text{on } \gamma_0 \\ [\mathbf{u}] = \mathbf{u}^+ - \mathbf{u}^- = \mathbf{g}_1 & \text{on } \gamma_1 \\ \sigma_0(\mathbf{u}_0)n - \sigma_1(\mathbf{u}_1)n = \mathbf{g}_1^n & \text{on } \gamma_1 \end{cases} . \tag{4.1}$$

The approximate solution of (4.1) is given by

$$\mathbf{u}_0(x) \approx \sum_{i=1}^{k} \alpha_i^0 \mathbf{\Phi}_{y_i}^0(x) := \widetilde{\mathbf{u}}_0(x), \quad x \in w_0$$

$$\mathbf{u}_1(x) \approx \sum_{i=1}^{n-k} \alpha_i^1 \mathbf{\Phi}_{y_{k+i}}^1(x) := \widetilde{\mathbf{u}}_1(x), \quad x \in w_1,$$

for some source points defined on the artificial boundaries: $y_1, ..., y_k \in \widehat{\gamma}_0 \cup \widehat{\gamma}_1$ and $y_{k+1}, ..., y_n \in \widehat{\Gamma}_1$, $(k > n)$. The vectorial coefficients $\alpha_i^0 = \left(\alpha_{i,1}^0,\ \alpha_{i,2}^0\right)$, $\alpha_i^1 = \left(\alpha_{i,1}^1,\ \alpha_{i,2}^1\right)$ are obtained by solving the least square system

$$\mathbf{A}^* \mathbf{A}\, \mathbf{X} = \mathbf{A}^* \mathbf{B}, \tag{4.2}$$

on some collocation points $x_1, x_2, ..., x_l \in \gamma_0$ and $x_{l+1}, x_{l+2}, ..., x_m \in \gamma_1$ $(m > l)$, where

$$\mathbf{A} = \begin{bmatrix} \mathbf{\Phi}_{y_1}^0(x_1) & \ldots & \mathbf{\Phi}_{y_k}^0(x_1) & 0 & \ldots & 0 \\ \ldots & & \ldots & 0 & \ldots & 0 \\ \mathbf{\Phi}_{y_1}^0(x_l) & \ldots & \mathbf{\Phi}_{y_k}^0(x_l) & 0 & \ldots & 0 \\ \mathbf{\Phi}_{y_1}^0(x_{l+1}) & \ldots & \mathbf{\Phi}_{y_k}^0(x_{l+1}) & \mathbf{\Phi}_{y_{k+1}}^1(x_{l+1}) & \ldots & \mathbf{\Phi}_{y_n}^1(x_{l+1}) \\ \ldots & & \ldots & & \ldots & \ldots \\ \mathbf{\Phi}_{y_1}^0(x_m) & \ldots & \mathbf{\Phi}_{y_k}^0(x_m) & \mathbf{\Phi}_{y_{k+1}}^1(x_m) & \ldots & \mathbf{\Phi}_{y_n}^1(x_m) \\ \sigma_0(\mathbf{\Phi}_{y_1}^0(x_{l+1}))n & \ldots & \sigma_0(\mathbf{\Phi}_{y_k}^0(x_{l+1}))n & -\sigma_1(\mathbf{\Phi}_{y_{k+1}}^1(x_{l+1}))n & \ldots & -\sigma_1(\mathbf{\Phi}_{y_n}^1(x_{l+1}))n \\ \ldots & & \ldots & & \ldots & \ldots \\ \sigma_0(\mathbf{\Phi}_{y_1}^0(x_m))n & \ldots & \sigma_0(\mathbf{\Phi}_{y_k}^0(x_m))n & -\sigma_1(\mathbf{\Phi}_{y_{k+1}}^1(x_m))n & \ldots & -\sigma_1(\mathbf{\Phi}_{y_n}^1(x_m))n \end{bmatrix}$$

and

$$\mathbf{B} = \left[\begin{array}{cccccccccc} \mathbf{g}_0(x_1) & \cdots & \mathbf{g}_0(x_l) & \mathbf{g}_1(x_{l+1}) & \cdots & \mathbf{g}_1(x_m) & \mathbf{g}_1^n(x_{l+1}) & \cdots & \mathbf{g}_1^n(x_m) \end{array} \right]^T.$$

In the numerical experiments we consider $n = 2m$. We define the following quantities

$$\|\mathbf{E}^0\|_\infty^m = \max_{i,j} \|\mathbf{u}_0(x_i, y_j) - \widetilde{\mathbf{u}}_0^m(x_i, y_j)\|_\infty, \text{ for } (x_i, y_j) \in w_0,$$
$$\|\mathbf{E}^1\|_\infty^m = \max_{i,j} \|\mathbf{u}_1(x_i, y_j) - \widetilde{\mathbf{u}}_1^m(x_i, y_j)\|_\infty, \text{ for } (x_i, y_j) \in w_1$$

and $\|\mathbf{E}\|_\infty^m = \max\{\|\mathbf{E}^0\|_\infty^m, |\mathbf{E}^1\|_\infty^m\}$, where $\widetilde{\mathbf{u}}_0^m(x)$ and $\widetilde{\mathbf{u}}_1^m(x)$ are the approximate solutions of $\mathbf{u}_0(x)$ and $\mathbf{u}_1(x)$, respectively, obtained by the MFS using m collocation points and $2m$ source points. In this section we consider three numerical examples.

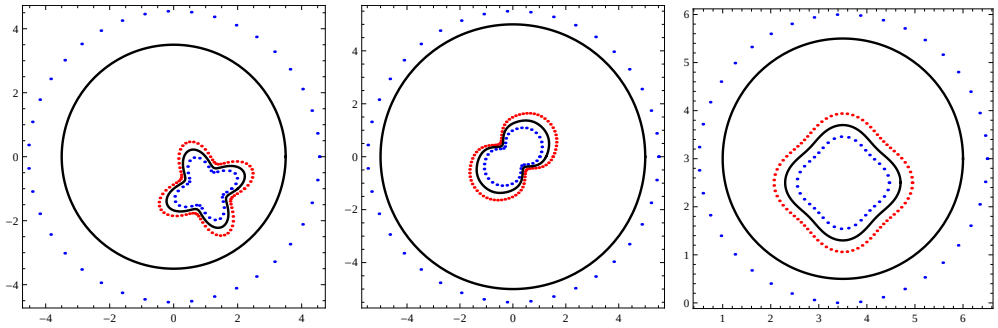

(a) Example 1 (b) Example 2 (c) Example 3

FIG. 4.1. *Geometry of the domains and the artificial boundaries. Boundaries γ_0 and γ_1 in black; source points defined on the artificial boundaries $\widetilde{\gamma}_0 \cup \widetilde{\gamma}_1$ and $\widetilde{\Gamma}_1$ in blue and red, respectively.*

Example 1: In this example we consider the problem (4.1) with

- $\Omega = \{(x,y) \in \mathbf{R}^2 : x^2 + y^2 < 3.5^2\}$,
- the interface γ_1 given by the parametrization

$$\varphi(t) = (1,-1) + (1 + 0.3\sin(4t))\,(\cos(t), \sin(t))\,, \quad 0 \le t \le 2\pi,$$

- $w_1 = \left\{(x,y) \in \mathbf{R}^2 : (x-1)^2 + (y+1)^2 < \rho(x,y)^2\right\}$, where $\rho(x,y) = 1.0 + 0.3\sin\left(4\arctan\left((y+1)/(x-1)\right)\right)$.

The Dirichlet boundary condition and the interface conditions are determined from the following exact solution,

$$\mathbf{u}(x,y) = \begin{cases} \mathbf{u}_0(x,y), & (x,y) \in w_0, \\ \mathbf{u}_1(x,y), & (x,y) \in w_1, \end{cases},$$

with

$$\begin{aligned} \mathbf{u}_0(x,y) = \Big(& -y(2x+y) - \exp(y)\sin(x) + \frac{\exp(x)}{\lambda_0+\mu_0}\left(\lambda_0 + 3\mu_0 + (\mu_0 - \lambda_0)x\right), \\ & \exp(y)\cos(x) - x\exp(x)\cos(y) + \frac{1}{\lambda_0+\mu_0}\left((\lambda_0+3\mu_0)x^2 + (\lambda_0-\mu_0)y^2 + 2\mu_0 xy\right)\Big), \\ & (x,y) \in w_0, \end{aligned}$$

$$\begin{aligned} \mathbf{u}_1(x,y) = \Big(& -2xy + \exp(x)\cos(y) - \frac{\exp(x)}{\lambda_1+\mu_1}\left((\lambda_1+\mu_1)x - \lambda_1 - 3\mu_1\right)\sin(y), \\ & \frac{1}{\lambda_1+\mu_1}\left((\lambda_1-\mu_1)y^2 + (\lambda_1+3\mu_1)x^2\right) - \exp(x)(x\cos(y) + \sin(x))\Big), \\ & (x,y) \in w_1, \end{aligned} \tag{4.3}$$

where the values of the Lamé constants are given by $\lambda_0 = 2.5,\ \lambda_1 = 5.2,\ \mu_0 = 6.5$ and $\mu_1 = 12$.

In Table 4.1 the first column m is the number of collocation points, the second column $Cond(A)$, identified as the condition number of the matrix $\mathbf{A}$, is given by $\|\mathbf{A}\|_2\|\mathbf{A}^+\|_2$, where $\mathbf{A}^+$ is the pseudoinverse of $\mathbf{A}$ and the third and fourth columns are the absolute errors in w_0 and w_1, respectively. The results presented in Table 4.1 show that the matrix $\mathbf{A}$ has, as expected, a very large condition number. However, is possible to obtain an approximate solution, of the problem (4.3), with a very small error $\|\mathbf{E}\|_\infty^m$, namely for $m = 640$ we have $\|\mathbf{E}\|_\infty^m \approx 10^{-12}$ near machine precision. In Figures 4.2(a) and 4.2(b) we present the absolute error for the MFS solution of (4.3) obtained with 640 collocation points and 1280 source points, and we observe that the maximum of the absolute error for both coordinates of the solution is less than 6×10^{-12}.

TABLE 4.1
Condition number, maximum of errors for Example 1.

m	$Cond(\mathbf{A})$	$\|\mathbf{E}^0\|_\infty^m$	$\|\mathbf{E}^1\|_\infty^m$
40	2.81057×10^6	2.86132×10^0	2.6406×10^0
80	1.46688×10^9	5.89266×10^{-2}	5.94683×10^{-2}
160	9.23019×10^{13}	9.81098×10^{-6}	2.08591×10^{-5}
320	4.10794×10^{14}	8.92367×10^{-10}	2.39192×10^{-9}
640	4.90659×10^{14}	4.23245×10^{-13}	4.33431×10^{-12}
800	7.74936×10^{14}	2.81997×10^{-13}	4.89209×10^{-12}

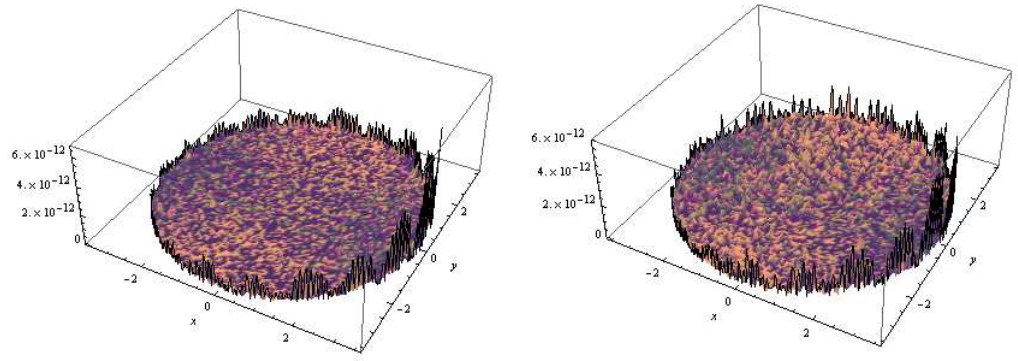

FIG. 4.2. *Example 1- Absolute error for each coordinate of the MFS approximation with 640 collocation points and 1280 source points. (a) Error for the first coordinate,* $|\mathbf{u}(x,y).e_1 - \widetilde{\mathbf{u}}(x,y).e_1|$. *(b) Error for the second coordinate,* $|\mathbf{u}(x,y).e_2 - \widetilde{\mathbf{u}}(x,y).e_2|$.

Example 2: In this example we consider (cf. Figure 4.1(b))

- $\Omega = \{(x,y) \in \mathbf{R}^2 : x^2 + y^2 < 5^2\}$,
- the interface γ_1 given by the parametrization

$$\varphi(t) = \rho(t)\,(\cos(t), \sin(t))\,, \quad 0 \le t \le 2\pi,$$

with $\rho(t) = \dfrac{105\pi + \sqrt{2}\,(315 + 42\cos(4t) - 10\cos(8t) + 210\sin(2t) - 18\sin(6t))}{210\pi}$.

- $w_1 = \left\{(x,y) \in \mathbf{R}^2 : x^2 + y^2 < \rho(\arctan(y/x))^2\right\}$.

The Dirichlet boundary condition and the interface conditions are determined from the following exact solution

$$\begin{aligned}
\mathbf{u}_0(x,y) = \Big(& -y(y-1) - \frac{\exp(x)\sin(y)}{\lambda_0+\mu_0}\left((x-1)\lambda_0 + (x-3)\mu_0\right), \\
& \frac{y(\lambda_0+\mu_0+2y\mu_0)}{\lambda_0+\mu_0} - x\exp(x)\cos(y)\Big), \\
& (x,y) \in w_0, \\
\\
\mathbf{u}_1(x,y) = \Big(& \frac{y(\lambda_1+\mu_1+2x\mu_1)}{\lambda_1+\mu_1} + y\sin(x)\exp(y), \\
& x(1-x) - \frac{\exp(y)\cos(x)}{\lambda_1+\mu_1}\left((y-1)\lambda_1 + (y-3)\mu_1\right)\Big), \\
& (x,y) \in w_1,
\end{aligned} \tag{4.4}$$

where the values of the Lamé constants are given by $\lambda_0 = 10,\ \lambda_1 = 25,\ \mu_0 = 15$ and $\mu_1 = 50$.

From the results listed in Table 4.2 we can see, like on the previous example, for each value of m we have a ill conditioned system of equations, the condition number of matrix $\mathbf{A}$ is large and increasing with m. However the MFS solution has small errors. For instance, when $m = 640$ we have $\|\mathbf{E}\|_\infty^m \approx 10^{-10}$. Figure 4.3 show plots of the absolute error to the MFS solution $\widetilde{\mathbf{u}}$ with $m = 640$. In Figures 4.4 and 4.5 we present the absolute error on each domain w_0 and w_1, that means, the absolute error for the MFS solutions $\widetilde{\mathbf{u}}_0$ and $\widetilde{\mathbf{u}}_1$, respectively. From Figure 4.5 we see that the maximum of the absolute errors to the MFS solution $\widetilde{u}_1$ is achieved near the boundary that defines

TABLE 4.2
Condition number, maximum of errors for Example 2.

m	$Cond(\mathbf{A})$	$\|\mathbf{E}^0\|_\infty^m$	$\|\mathbf{E}^1\|_\infty^m$
40	7.33891×10^5	1.21219×10^0	4.91204×10^1
80	1.4063×10^7	7.98405×10^{-2}	8.77217×10^{-1}
160	1.47196×10^{11}	2.16442×10^{-5}	4.48811×10^{-4}
320	3.75166×10^{13}	6.34955×10^{-9}	1.37902×10^{-10}
640	4.30366×10^{13}	1.47982×10^{-12}	9.04521×10^{-11}

the interface. We have a similar situation for the absolute error to the MFS solution $\widetilde{u}_0$, the maximum of the absolute error is obtained near the boundary of Ω (see Figure 4.4).

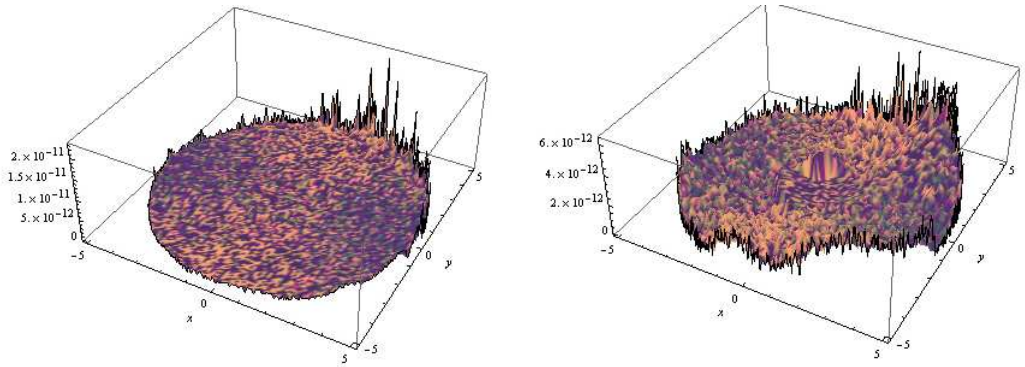

(a) (b)

FIG. 4.3. *Example 2- Absolute error for each coordinate of the MFS solution* $\widetilde{\mathbf{u}}$ *with 640 collocation points and 1280 source points. (a) Error for the first coordinate,* $|\mathbf{u}(x,y).e_1 - \widetilde{\mathbf{u}}(x,y).e_1|$. *(b) Error for the second coordinate,* $|\mathbf{u}(x,y).e_2 - \widetilde{\mathbf{u}}(x,y).e_2|$.

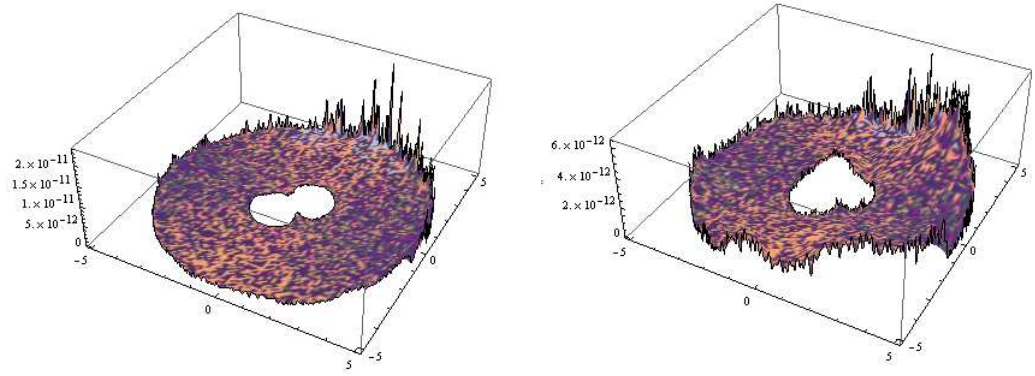

(a) (b)

FIG. 4.4. *Example 2- Absolute error for each coordinate of the MFS with with 640 collocation points and 1280 source points, on domain* w_0. *(a) Error for the first coordinate,* $|\mathbf{u}_0(x,y).e_1 - \widetilde{\mathbf{u}}_0(x,y).e_1|$—. *(b) Error for the second coordinate,* $|\mathbf{u}_0(x,y).e_2 - \widetilde{\mathbf{u}}_0(x,y).e_2|$.

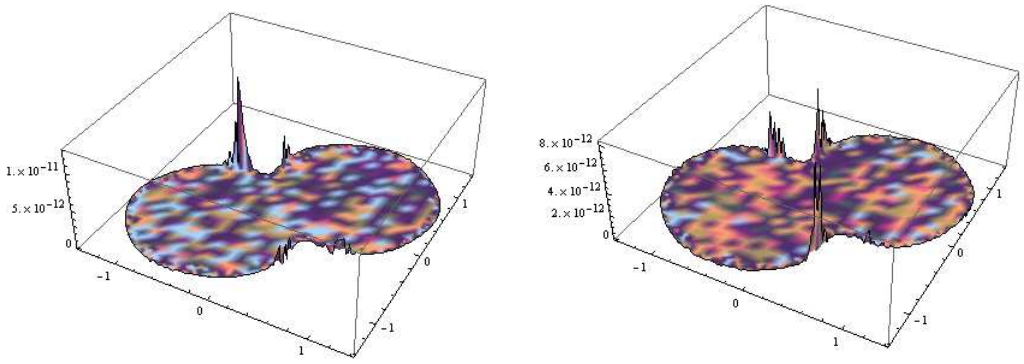

(a) (b)

FIG. 4.5. *Example 2- Absolute error for each coordinate of the MFS solution with with 640 collocation points and 1280 source points, on the interior of the interface* γ_1. *(a) Error for the first coordinate,* $|\mathbf{u}_1(x,y).e_1 - \widetilde{\mathbf{u}}_1(x,y).e_1|$. *(b) Error for the second coordinate,* $|\mathbf{u}_1(x,y).e_2 - \widetilde{\mathbf{u}}_1(x,y).e_2|$.

Example 3: In the last example we consider the domain Ω, the interface γ_1 and the domain w_1 defined as follows (cf. Figure 4.1(c)).

- $\Omega = \{(x,y) \in \mathbf{R}^2 : (x-3.5)^2 + (y-3)^2 < 2.5^2\}$,
- γ_1 is given by the parametrization

$$\varphi(t) = (3.5, 2.5) + \left(1 + 0.2\cos(2t)^2\right)(\cos(t), \sin(t)), \quad 0 \le t \le 2\pi,$$

- $w_1 = \left\{(x,y) \in \mathbf{R}^2 : (x-3.5)^2 + (y-2.5)^2 < \rho(x,y)^2\right\}$, with

$$\rho(x,y) = 1.0 + 0.2\cos\left(2\arctan\left((y-2.5)/(x-3.5)\right)\right)^2.$$

The Dirichlet boundary condition and the interface conditions are determined from the following exact solution

$$\begin{aligned}
\mathbf{u}_0(x,y) = \Big(& \frac{1}{r^2\beta_0}\left(y^2(\beta_0 + y(\lambda_0 + 3\mu_0)) + x^2(-\beta_0 + y(3\lambda_0 + 5\mu_0)) + e^y y r^2 \beta_0 \sin(x)\right), \\
& \frac{x\left(-x^2 + (y-2)y\right)}{r^2} - \frac{1}{\beta_0} e^y (y\beta_0 - \lambda_0 - 3\mu_0)\cos(x)\Big), \\
& (x,y) \in w_0, \\
\mathbf{u}_1(x,y) = \Big(& -y^2 - \frac{2x(x+y)}{r^2} + \frac{1}{r} - \frac{1}{\beta_1} e^x((-1+x)\lambda_1 + (-3+x)\mu_1)\sin(y) \\
& -2xy - \frac{2y(y+x)}{r^2} + \frac{1}{r} + \frac{2xy(\lambda_1 + 2\mu_1)}{\beta_1} - e^x x\cos(y)\Big), \\
& (x,y) \in w_1,
\end{aligned} \tag{4.5}$$

where $r = x^2 + y^2$, $\beta_i = \lambda_i + \mu_i$, $i = 0, 1$.

The purpose of this example is consider several values for the Lamé coefficients λ_0, μ_0 (small and large values) and analyse the absolute errors of the MFS solutions. In this example we scale $\|E\|_\infty^m$, as follows to get the relative errors

$$r_\infty^m = \frac{\|\mathbf{E}\|_\infty^m}{\max_{i,j} \|\mathbf{u}(x_i, y_j)\|_\infty}.$$

In Table 4.3 we list, for several values of m, the condition number of the matrix $\mathbf{A}$ in the sense of the pseudoinverse matrix, $Cond(\mathbf{A}) = \|\mathbf{A}\|_2 \|\mathbf{A}^+\|_2$, the absolute errors $\|\mathbf{E}\|_\infty^m$ and the relative errors r_∞^m for the MFS solution of (4.5) (for several values of λ_0 and μ_0). We note that for the cases when the Lamé coefficients λ_0, μ_0 has the large and small values the absolute error is bigger. However the condition number of the matrix $\mathbf{A}$ has similar values for all the values of λ_0, μ_0.

5. Conclusions.

In this paper, we have proposed a meshfree method based on fundamental solutions basis functions for solving a linear elasticity problem with interfaces. The main idea of these methods is to consider representations of the solution as a linear combination of point source fundamental tensors centered at some points placed outside the domain of interest (cf. (3.4)-(3.5)). The vectorial coefficients of these linear combinations can be computed by imposing, on some boundary points (collocation points), the boundary conditions of the transmission problem. We presented injectivity and density results in order to justify the proposed method. Several numerical examples in 2D domains were presented in order to show the accuracy and feasibility of the method. Overall, we obtained good results for smooth domains and smooth boundary data. Possible extensions to the 3D problem require only surface discretizations and are straightforward.

TABLE 4.3
Condition number, maximum of errors and relative errors for Example 3 with $\lambda_1 = \mu_1 = 10$ and several values of the Lamé coefficients $\lambda_0,\ \mu_0$.

	$\lambda_0 = 10,\ \mu_0 = 5$			$\lambda_0 = 1000,\ \mu_0 = 5000$		
m	$Cond(\mathbf{A})$	$\|\mathbf{E}\|_\infty^m$	r_∞^m	$Cond(\mathbf{A})$	$\|\mathbf{E}\|_\infty^m$	r_∞^m
40	1.00770×10^5	5.09696×10^0	5.78813×10^{-3}	9.20707×10^7	1.58734×10^1	3.51017×10^{-2}
80	3.98901×10^6	3.21298×10^{-3}	3.64867×10^{-6}	4.15415×10^9	1.77547×10^{-3}	2.53424×10^{-6}
160	7.63681×10^{10}	3.01274×10^{-7}	6.66225×10^{-10}	1.25902×10^{13}	2.72164×10^{-7}	6.01853×10^{-10}
320	4.33864×10^{13}	3.09228×10^{-11}	3.51161×10^{-14}	4.49825×10^{13}	2.05168×10^{-8}	4.537×10^{-11}
640	4.29489×10^{13}	3.24434×10^{-11}	3.68428×10^{-14}	4.29489×10^{13}	5.17174×10^{-9}	7.38194×10^{-12}
	$\lambda_0 = 0.1,\ \mu_0 = 0.5$			$\lambda_0 = 0.0001,\ \mu_0 = 0.0005$		
m	$Cond(\mathbf{A})$	$\|\mathbf{E}\|_\infty^m$	r_∞^m	$Cond(\mathbf{A})$	$\|\mathbf{E}\|_\infty^m$	r_∞^m
40	3.84064×10^4	1.33479×10^2	2.95169×10^{-1}	3.18481×10^5	2.25465×10^2	4.98584×10^{-1}
80	5.50975×10^6	1.32662×10^{-2}	2.90369×10^{-5}	3.68906×10^8	1.54663×10^2	3.42016×10^{-1}
160	4.81489×10^{10}	3.50037×10^{-7}	7.74058×10^{-10}	2.32623×10^{13}	9.87367×10^{-6}	2.18342×10^{-8}
320	4.17899×10^{13}	1.31593×10^{-11}	1.8783×10^{-14}	4.50297×10^{13}	2.46195×10^{-9}	5.38905×10^{-12}
640	4.06605×10^{13}	1.74225×10^{-11}	2.48682×10^{-14}	4.50166×10^{13}	9.2848×10^{-9}	1.32528×10^{-11}

Acknowledgments. The second author acknowledge support from Fundação para a Ciência e a Tecnologia, Portugal, through Project PTDC/MAT/101867/2008.

REFERENCES

[1] C.J.S. ALVES, *Preface to the special issue on meshless methods*, Eng. Anal. Boundary Elem. 32 No. 6, (2008).
[2] C.J.S. ALVES, *On the choice of source points in the method of fundamental solutions*, Eng. Anal. Boundary Elem. 33 (2009), pp. 1348–1361.
[3] C.J.S. ALVES AND C.S. CHEN, *A new method of fundamental solutions applied to non-homogeneous elliptic problems*, Advances in Computational Mathematics 23 (2005), pp. 125–142.
[4] C.J.S. ALVES AND N.F.M. MARTINS, *The direct method of fundamental solutions and the inverse Kirsh-Kress method for the reconstruction of elastic inclusions or cavities*, J. Integral Equations and Applications, 21, N. 2, (2009), pp. 153–178.
[5] G. CHEN AND J.ZHOU, *Boundary element methods*, Academic Press, London, (1992).
[6] G.E. FASSHAUER, *Meshfree methods*, Handbook of Theoretical and Computational Nanotechnology, M. Rieth and W. Schommers (eds.), American Scientific Publishers, vol. 2 (2006), pp. 33–97.
[7] A. KARAGEORGHIS, D. LESNIC AND L. MARIN, *A survey of applications of the MFS to inverse problems*, Inverse Problems in Science and Engineering 19 No. 3 (2011), pp. 309–336.
[8] Y.LIU, L. Z. SUN AND G. WANG, *Tomography based 3-D anisotropic elastography using boundary measurements*, IEEE Transactions on Medical Imaging, Vol. 24, N. 10, (2003), pp. 1323–1333.
[9] E.J. KANSA, *Multiquadrics - A scattered data approximation scheme with applications to computational fluid-dynamics - II: Solutions to parabolic, hyperbolic and elliptic partial differential equations*, Comput. Math. Appl., 19 (1990), pp. 147–161.
[10] V.D. KUPRADZE AND M.A. ALEKSIDZE, *The method of functional equations for the approximate solution of certain boundary value problems*, USSR Computational Mathematics and Mathematical Physics 4, (1964), pp. 82–126 .
[11] W. MCLEAN, *Strongly Elliptic Systems and Boundary Integral Equations*, Cambridge University Press, (2000).
[12] E.R. ARANTES E OLIVEIRA, *Plane stress analysis by a general integral method*, Proc. ASCE Eng. Mech. Div. 94,(1968) , pp. 79–101.
[13] X.YANG, B. LI AND Z. LI, *The immersed interface method for elasticity problems with interface*, Dynamics of Continous Discrete and impulsive Systems 10, (2003), pp. 783–808.
[14] H. XIE, Z. LI AND Z. QIAO, *A finite element method for elasticity interface problems with*

locally modified triangulations, International Journal of numerical analysis and modeling 8, (2011), pp.189–200.